Cyclic Behaviour of RC Columns Confined with Steel Reinforced Polymer Wraps

15 WCEE
LISBOA 2012

P. Casadei
Fidia S.r.l. - Technical Global Services, Perugia, Italy

C. Faella, A. Napoli, F. Perri & R. Realfonzo
University of Salerno, Italy

J. G. Ruiz Pinilla
Universitat Politècnica de València, ICITECH, Spain

SUMMARY
This paper presents the first results of an experimental campaign undertaken to investigate the seismic behaviour of full scale square (300x300 mm) and rectangular (300x700 mm) RC columns externally strengthened with Steel Fiber Reinforced Polymer (SFRP) wraps. Studied columns were designed to be representative of existing building structural components. For this reason, they were realized with medium-low concrete strength and were reinforced using smooth steel rebars; the reinforcement details were arranged by following design rules used in the past and without keeping into account any seismic details.
The first performed tests, all relative to square columns, have allowed to investigate the influence of a SFRP strengthening system on the specimen performance mainly in terms of flexural strength and ductility. The benefits achievable with this technique are also compared with those of companion specimens strengthened with carbon Fiber Reinforced Polymer layers, whose results have been already published elsewhere.

Keywords: column, steel fiber reinforced polymers, experimental tests, strength, ductility

1. INTRODUCTION

Recent earthquakes have frequently evidenced the vulnerabilities of existing reinforced concrete (RC) structures to seismic deformation and shear demands.
It is known that the most building heritage built prior to the 1970s was designed in order to withstand only gravity loads or according to outdated seismic rules. In particular, these “under designed” structures are often characterized by an unsatisfactory weak column-strong beam behaviour that, under a seismic event, yields most likely to the formation of local hinges in the columns and to a consequent low available global ductility.
In order to improve the strength and mainly the ductility of under-designed RC columns, external confinement systems employing fiber reinforced polymer (FRP) materials have emerged as a promising alternative to the traditional strengthening techniques, such as steel or concrete jacketing.
The use of FRP confining systems does not allow, except for particular cases, to convert the local collapse mechanism in a global one (strong column-week beam behaviour); however, it assures a greater availability of global ductility by increasing the local one.
Typically, FRP confinement systems employ carbon (CFRP), glass (GFRP) and aramid (AFRP) fibers. The effectiveness of using these materials has been widely investigated in the literature by testing both small and full scale FRP-confined concrete specimens in either uniaxial compression or combined axial load and cyclic flexure. Additionally, several analytical models able to predict the compressive strength, the corresponding ultimate axial strain and the stress-strain constitutive law of the FRP confined concrete have been developed; advanced states of the art on the mentioned topics can be found in Teng et al. (2002) and Realfonzo and Napoli (2011). National and International design guidelines are also available (CNR-DT200/2004; *fib* bulletin n.14 2001; ACI 440.2R-08).
Recently, a new class of composites made of steel FRP (SFRP) materials has emerged as a promising and cost-effective solution for external confinement of concrete members. The SFRP sheet consists of high carbon steel cords made by twisting steel wires instead of carbon/glass fibers; it can be applied to

the structural member according to a wet lay-up installation procedure.

To date, the literature related to SFRP confined concrete is very limited. Only recently, few researchers have experimentally investigated the effectiveness of this strengthening system. Among them, El-Hacha and Mashrik (2012), performed several monotonic compression tests on small scale plain concrete members confined with SFRP jackets; the main study parameters were: the number of SFRP layers, the shape of the cross-section (circular and square), the concrete strength and the corner radius for square columns. Abdelrahman and El-Hacha (2011), instead, investigated the behaviour in uniaxial compression of non-reinforced and reinforced large scale columns wrapped with SFRP sheets; they observed an improved performance with respect to that of CFRP confined members.

However, if the response under compression has been recently explored, there is no current research available in the literature on the behaviour of full scale SFRP confined RC columns subjected to axial load and cyclic flexure. As such, the effectiveness of SFRP as strengthening material to confine concrete needs to be addressed and studied extensively.

With the aim to fill these knowledge gaps, an experimental campaign is in progress at the Laboratory of Materials & Structures of the University of Salerno (Italy) to investigate the cyclic performance of full scale RC columns strengthened with SFRP systems. The test matrix includes eight 300 x 300 mm square columns and five 300 x 700 rectangular members realized with medium-low concrete strength and reinforced using smooth steel rebars; the reinforcement details were arranged by following design rules used in the past and without keeping into account any seismic details.

Two SFRP strengthening systems were investigated: the former characterized by only external SFRP confinement, while the latter consisted of both SFRP confinement and longitudinal reinforcement anchored to the foundation.

Four tests have been performed so far, all relative to square columns. The obtained results have allowed to preliminary investigate the influence of the SRP strengthening system on the specimen performance mainly in terms of flexural strength and ductility. The benefits achievable with this technique have been compared with those of companion specimens confined with CFRP layers, whose results have been already published elsewhere (Realfonzo and Napoli 2009).

2. EXPERIMENTAL CAMPAIGN

The experimental campaign, still ongoing at the Laboratory of Materials & Structures of the University of Salerno, includes 13 full scale RC columns subjected to a constant axial load and a cyclically reversed horizontal force. Of these, eight specimens have a square 300x300 mm^2 cross section, a length of 2200 mm and a concrete foundation of dimensions 1400 x 600 x 600 mm; the remaining ones, instead, have a rectangular 300x700 mm^2 cross section, a length of 2500 mm and a concrete foundation of dimensions 1400 x 600 x 800 mm.

All specimens were designed and realized to be representative of structural components belonging to gravity load designed existing buildings. For this reason, they were realized by using a medium-low strength concrete; in particular, the concrete mixture was designed in order to obtain a mean value of the cylindrical compression strength, f_{cm} (= $0.83 \cdot R_{cm}$, where R_{cm} is the cubic one) ranging from about 10 to 18 MPa. The actual value of the concrete strength per each column was estimated by testing in compression a set of three 150 mm edge cubic samples, cast along with the column and cured under the same environmental conditions. Also, the longitudinal steel reinforcement of members consisted of smooth steel rebars, as frequently used in the past, which always overlapped at the column-base joint for a length ranging from about 30 to 40 diameters.

Four tests have been performed so far, all relative to square columns and the results are presented and discussed herein. The following sections provide a detailed description about the eight specimens involved in this first phase of the experimental campaign, the strengthening layouts and the test set-up.

2.1. Test specimens and strengthening layouts

Figure 1 illustrates the geometry and the steel reinforcement configurations adopted for the eight 300 x 300 mm^2 square specimens; of these, four columns were realized according to the scheme "*type 1*" (Fig. 1a) and four by following the drawing "*type 2*" (Fig. 1b). In the two schemes, the columns have

the same amount of longitudinal steel reinforcement, consisting of six rebars with a 14 mm diameter (3+3 Φ14) but with different anchorage details in the overlapping area at the column-base joint. In particular, the steel reinforcement in the "Type 2" is characterized by a lap splice length of about 30 diameters and does not have proper end-anchorages; in the "Type 1" instead, the details were realized according to the old italian code provisions, with an overlapping length of about 40 bar diameters and 50-mm radii hooks as end-anchorages.
The average values of the mechanical properties of these rebars, as obtained by tensile tests, are: yielding strength, f_{sy} = 390 MPa and corresponding strain, ε_{sy} = 0.186%; ultimate strength, f_{su} = 454 MPa and corresponding strain, ε_{su} = 35%.
The transverse reinforcement consisted of 8 mm diameter steel stirrups, 200 mm spaced and closed with 90-degree hooks at both ends; the spacing was reduced to 50 mm only in the region of the column involved by the application of the horizontal force.

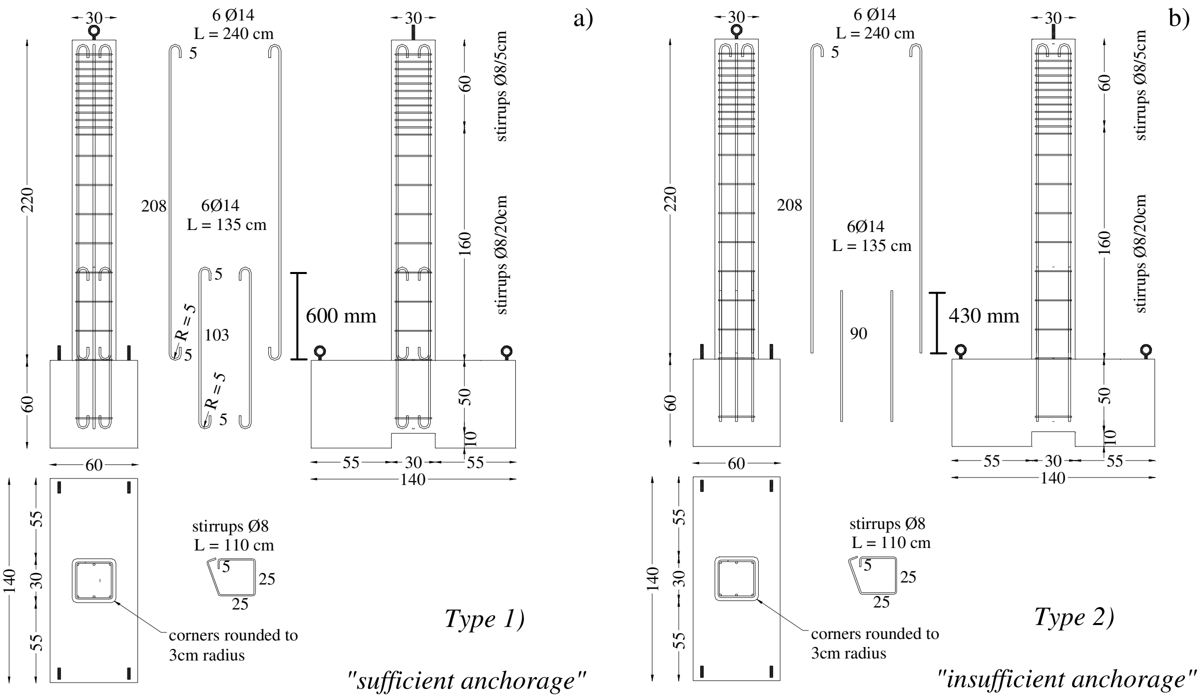

Figure 1. Geometry and configuration of steel rebars with: sufficient (a) and insufficient anchorage (b).

The systems used for strengthening the test specimens are shown in Figure 2.
The type "A" system (Fig. 2a) consisted of a passive confinement realized by wrapping members with unidirectional SFRP layers. In particular, starting from the column base, the first portion of the member (≈500 mm) was continuously confined, while the remaining part was strengthened by means of 150 mm spaced strips, each having a width of 100 mm. The strengthening layout is the same already used in a previous experimental campaign (Realfonzo and Napoli 2009) where the column jacket was realized by using carbon FRP sheets. With the aim to better compare the performances of members strengthened by using two alternative materials, three SFRP layers were employed to obtain a jacket extensional stiffness comparable to that of two high modulus carbon FRP layers used in the experimental campaign. In particular, Hardwire® steel fiber sheets with medium (1 layer) and high (2 layers) density were selected; the thickness and mechanical properties of these materials, as provided by the supplier, are reported in Table 1; where: t_{SFRP} is the sheet equivalent design thickness, f_{SFRP} the ultimate tensile strength, E_{SFRP} the elastic modulus and $\varepsilon_{SFRP,u}$ the ultimate strain.

Table 1. Thickness and mechanical properties of SFRP sheets.

Hardwire® steel fiber	density	t_{SFRP}	f_{SFRP}	E_{SFRP}	$\varepsilon_{SFRP,u}$
		(mm)	(MPa)	(GPa)	(%)
FIDSTEEL 3X2-B12	medium	0.227	3070	190	1.60
FIDSTEEL 3X2-B20	high	0.378			

In order to prevent stress concentrations – which may cause the premature failure of the SFRP system – the column corners were rounded to a radius of approximately 30 mm before applying the jacket.
The type “B” system (Fig. 2b), instead, employed a layer of longitudinal SFRP high density sheet (200 mm wide) on two opposite column sides before applying the same external wrapping of the layout "A". The anchorage of the longitudinal sheet to the foundation was made by using four (two per column side) FIDSTEEL mono thread connectors obtained by an high density SFRP sheet, 150 mm wide; the rigid portion of each connector, approximately 400 mm long, was restrained within the concrete foundation by using epoxy adhesive.

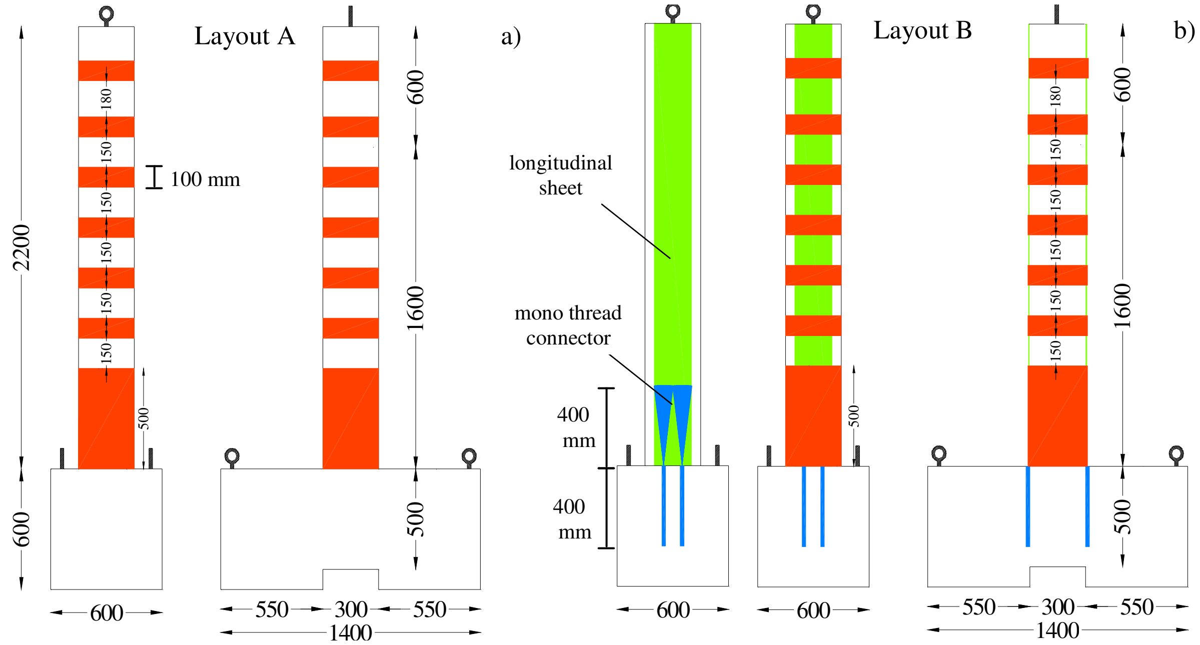

Figure 2. SFRP strengthening layouts: only confinement (a); confinement and longitudinal reinforcement (b)

2.2. Test set-up and instrumentation

The test set-up is shown in Fig. 3; it is very similar to that already used in the previous experimental campaign (Realfonzo and Napoli 2009). Columns were mounted vertically and tested under combined axial and lateral loads. They were restrained to the lab’s floor by means of a steel system which consisted of: a) two transverse beams placed on the RC foundation and fixed to the floor by means of four high strength thread rods that were properly pre-tensioned in order to avoid any stub rotation; b) two stiff steel plates fixed onto the ground and placed orthogonally to the load direction at the stub bottom in order to prevent any horizontal movement.
The axial load (N) was applied before the horizontal one by pre-tensioning a pair of 32 mm diameter high strength steel rods with a 2000 kN MOOG hydraulic actuator: this actuator, placed at the top of the column, kept the axial load constant during each test. In particular, a value of the normalized compression load “ν” equal to 0.40 was considered, which is given by $N/(A_g\,f_{cm})$, being A_g the area of the column cross-section.
The horizontal action, instead, was cyclically applied in displacement control by using a 250kN MTS hydraulic actuator, mounted at 1700 mm from the column base and fixed to a reaction steel frame. An increment of the imposed horizontal displacement every three cycles was considered in order to evaluate the strength and stiffness degradation at repeated lateral load reversals.
After initial cycles at 1, 2, 4 and 6 mm, the displacement amplitude was given as fraction of the estimated tip yield displacement of the column, Δ_y (≈ 20 mm); two different displacement rates were considered during the tests: 0.1 mm/s before the achievement of Δy and 1 mm/s after Δy.
Tests were stopped well beyond a predetermined "conventional collapse" corresponding to the 15% strength degradation evaluated on the monotonic envelope of the load-displacement curves.
Loads, strains, displacements and crack widths were measured during the tests; in particular:
a) horizontal and vertical strains were monitored using several strain gauges placed on the column at

about 100 mm from the stub interface;
b) further gauges monitored the strains of the steel stirrup placed at about 200 mm from the column base and those of the steel longitudinal rebars inside and outside the overlapping region;
c) LVDTs were used to measure potential rigid stub displacements;
d) a wire transducer was used to measure lateral displacements at 1700 mm from the column base (i.e. where the lateral load is applied);
e) vertical displacements and crack widths at the column-stub interface were monitored by two potentiometers for each side placed at about 100 mm from the base; one of them had the pin located at 30 mm from the column base: in this way, the difference between the readings of two LVDTs allowed estimating the crack opening at the base and the slip of the rebars.

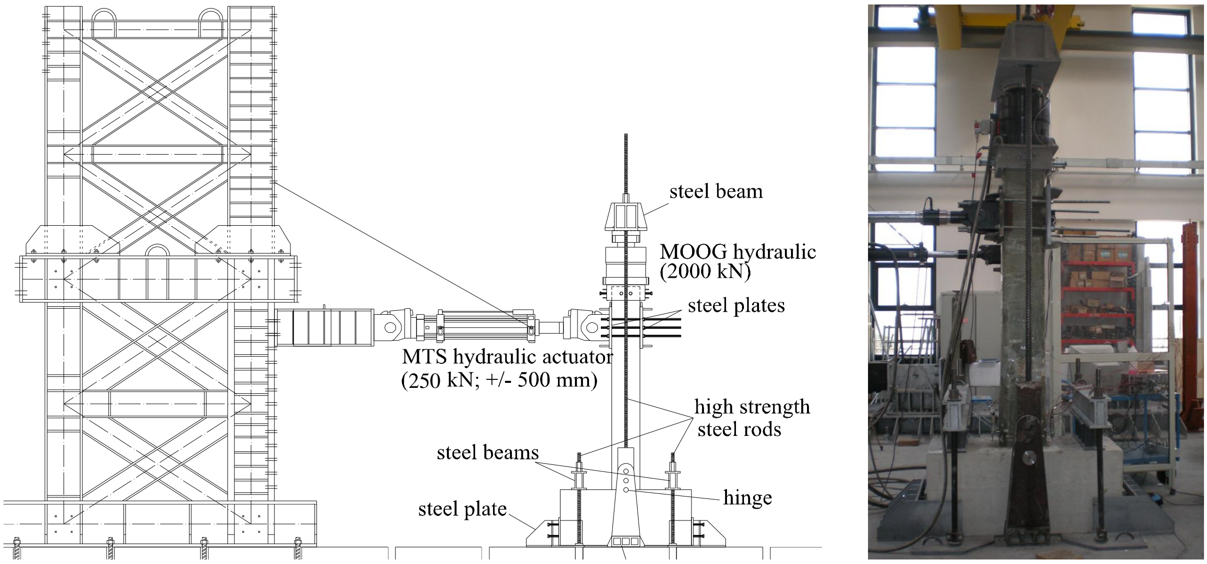

Figure 3. Test set-up

3. EXPERIMENTAL RESULTS

Table 2 summarizes the main data and results of the four tests performed so far, labeled: US1, A1, US2 and B2. In particular, US1 and A1 refer to columns characterized by "sufficient" overlapping length of rebars (i.e. specimens *type 1* in Fig. 2); the former is unstrengthened, while the latter is strengthened by only SFRP external confinement (see layout *A* in Fig.2). The labels US2 and B2, instead, identify two columns characterized by "insufficient" overlapping length of rebars (i.e. specimens *type* 2 in Fig. 2); the first one is unstrengthened, while the second one is upgraded by both external confinement and longitudinal flexural reinforcement (see layout *B* in Fig.2).
For each test, Table 2 reports: the value of f_{cm}; the applied axial load (N) corresponding to the normalized value $\nu = 0.40$; the peak lateral strengths in the two directions of loading (F^{+}_{max} and F^{-}_{min}) and the corresponding displacements (Δ^{+} and Δ^{-}); the maximum displacements of the column ($\Delta^{+}_{85\%}$ and $\Delta^{-}_{85\%}$) measured at the conventional collapse (i.e. at the achievement of 15% strength degradation evaluated on the horizontal force-displacement F-Δ curve); the observed failure modes.

Table 2. Test results and failure modes.

Test	f_{cm}	N	F^{+}_{max}	F^{-}_{max}	Δ^{+}	Δ^{-}	$\Delta^{+}_{85\%}$	$\Delta^{-}_{85\%}$	Failure mode
	(MPa)	(kN)	(kN)	(kN)	(mm)	(mm)	(mm)	(mm)	
US1	17.9	640	56.9	-56.4	20	-20	40	-40	Concrete spalling
A1	16.2	580	63.6	-61.1	100	-70	200	-180	wide crack at column base, damage in the unconfined region
US2	10.1	400	27.5	-33.9	10	-20	55.5	-66.3	Concrete spalling and crushing, rebar buckling
B2	10.5	400	55.8	-62.2	100	-70	160	-153.6	wide crack at column base, damage in the unconfined region, slip of SFRP connectors

By comparing the performances of the columns US1 and A1, for which the concrete strength is approximately the same, it is shown that the SFRP confinement system allows to considerably increase the ductility but not the flexural strength. As shown, the displacements exhibited by the specimen A1 at the achievement of the conventional collapse are almost five times over those measured for the counterpart US1; conversely, the increase of flexural strength is only 10%.
By comparing the performances of the columns US2 and A2, with comparable f_{cm} values, it is observed that the strengthening *type B* is able to almost double the flexural capacity of the unconfined member; a significant improvement of the deformation capacity, although lower than that experienced for the column A1, is also obtained, with a percentage increase over the member US2 of about 160%.

3.1. Cyclic behavior

Fig. 4 shows the lateral force (F)-tip displacement (Δ) cyclic curves of tested specimens which allow to better understand the effectiveness of the selected strengthening systems. In particular, Fig. 4a depicts the comparison between columns US1-A1, while Fig. 4b that of the specimens US2-A2. It is highlighted that the test US1 was stopped just beyond the achievement of the conventional collapse in order to not subject the member to severe damage and re-tested it once repaired and SFRP retrofitted.
It is noted that, the "pinching effect" typically characterizing the behavior of smooth rebars (Realfonzo and Napoli 2009), is mitigated in the case of SFRP strengthened members (compare US1 and A1).
By comparing the cyclic responses of specimens A1 and B2, it is observed that, after the peak flexural strengths are achieved, the former member is able to undergo significant lateral deformations without significantly reducing the flexural capacity. The specimen B2, instead, exhibits a more degrading behaviour which leads to a faster achievement of the conventional collapse; this evidence may be due to both the low concrete strength (f_{cm} = 10.5 MPa) and the reduced performance of the longitudinal SFRP reinforcement caused by the premature slippage of the steel connectors from the foundation.

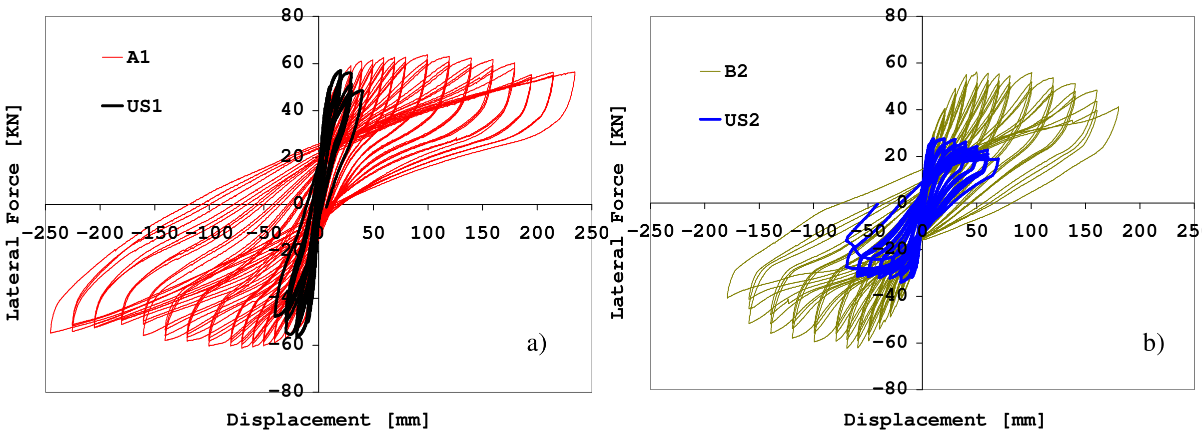

Figure 4. Lateral load – displacement cyclic curves

The performances of the tested members can be better compared through the normalized bending moment values "μ", which allow to by-pass the dependence of test results on the concrete strength level, thus providing a more immediate comparison of results in terms of flexural strength.
The normalized bending moment is given by:

$$\mu = \frac{F \cdot L_s}{B \cdot H^2 \cdot f_{cm}} = \frac{M}{B \cdot H^2 \cdot f_{cm}} \tag{3.1}$$

where: B and H are the width and the depth of the column cross section, respectively; F is the horizontal force applied by the MTS actuator, while L_s is the shear span of the column (L_s=1700 mm).
Fig. 5a depicts the relationships between the normalized flexural strength μ and the drift ratio δ (Δ/L_s).
The comparisons provide a clear overview about the efficiency of the strengthening systems and the influence of the steel rebars anchorage detailing on the member response. In the case of

unstrengthened members, an "adequate" anchorage only slightly increases the flexural strength, contrarily to what generally expected; however, this may also be due to the high value of axial force (ν = 0.40) chosen for these tests.
The efficiency of using the longitudinal SFRP reinforcement to improve the flexural capacity of members is well evidenced by comparing tests A1 and B2: an average increase of μ equal to about 45% is computed for the specimen B2 with respect to the SFRP confined counterpart.
Finally, the μ-δ envelopes of the members are compared in Fig. 5b with the experimental responses of three columns, labeled "C18-S", "C19-S-C" and "C20-S-A1", tested in the previous experimental campaign (Realfonzo and Napoli 2009). The three considered specimens were reinforced by using smooth steel rebars arranged according to the "*type 1*" configuration (Fig. 1a). Except for the control (unstrengthened) member C18-S, the others were externally strengthened with different CFRP systems. In particular, the member C19-S-C was externally confined by employing four CFRP layers according to the layout "*A*" of Fig. 2a. The strengthening system of the member C20-S-A1 also entailed longitudinal steel profiles (80x80x6 L-shape) along the column corners before applying the external wrapping made of two CFRP layers; each profile was anchored to the concrete foundation through a proper steel system.
Although the limited number of tests performed so far does not allow to perform an exhaustive analysis about the effectiveness of the considered strengthening techniques, the comparisons of Fig. 5b highlight the following aspects:
– the external confinement obtained by employing three SFRP layers allow to achieve a better performance in terms of ductility than a CFRP jacket of double extensional stiffness (in fact, the three SFRP layers are approximately equivalent to two used CFRP layers); however, the SFRP confinement is not sufficient by itself to significantly increase the flexural strength as already experienced for the CFRP jacket (compare tests A1 and C19-S-C);
– the use of a SFRP system *"type B"* does not allow to achieve strengths comparable to those experienced when using CFRP confinement and steel profiles (compare tests B2 and C20-S-A1); nevertheless, the increase of strength over the unstrengthened member is still significant;
– as expected, the performance of the specimen US1 is very similar to that of the specimen C18-S thus highlighting the reliability of the performed tests.

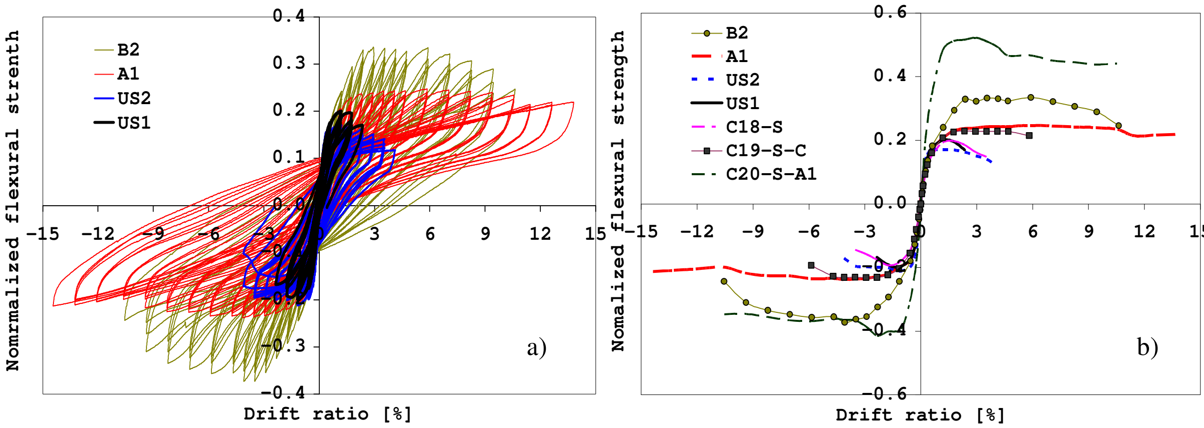

Figure 5. Dimensionless flexural resistance-drift ratio responses: cyclic curves (a); evelopes (b).

3.2. Failure mode

Disregarding the detailing of the steel reinforcement (*"insufficient"* or *"sufficient"* anchorage), unstrengthened members US1 and US2 exhibited cracking phenomena and significant damages concentrated in the first 500 mm from the column base (see Figs. 6-7).
In both cases, a flexural crack first developed at the column-foundation interface during an imposed displacement of 20 mm; the width of this crack did not significantly increase during the tests. Lacking adequate confinement, the columns were rapidly involved by the development of vertical cracks due to the incipient buckling of steel rebars which was in turn accompanied by concrete spalling.
Fig. 7c shows the relevant damage experienced by the column US2, for which the test was stopped

well beyond the achievement of the conventional collapse; crushing of concrete, buckling of rebars and stirrups opening are evidenced.

Regardless of the steel reinforcement detailing and strengthening layout (type A or B), the presence of a SFRP jacket has allowed to: a) inhibit the crack opening; b) avoid the crushing of concrete cover and the subsequent buckling of longitudinal rebars. The crack pattern of the specimens A1 and B2 was always characterized by the opening of a flexural crack at the column-stub interface, whose width significantly increased during the tests, and by further signs of damage at about 500-600 mm from the column base.

Figures 8a,b show the damage exhibited by the specimen A1. In particular, Fig. 8a shows the typical cracks occurred in the first unconfined portion of the column placed above the 500 mm continuous wrapping. These cracks, initially involved only the epoxy resin layer accumulated on the concrete member; at increasing the imposed displacement, the splitting of resin in that zone caused a slight damage of the surrounding concrete. Fig. 8b, instead, highlights the significant width of the flexural crack at the base under large column deformations (Fig. 8c). This implies that the behaviour of the member A1 was mainly characterized by a rigid rotation due to the slippage and elongation of steel rebars at the column-foundation interface, i.e. where the crack is located.

Finally, Fig. 9 shows the damage exhibited by the specimen B2. In this case, the splitting of the epoxy resin (Fig. 9a) accumulated on the concrete member severely cracked the concrete in that zone. Due to the significant damage of concrete by flexure-compression, the SFRP reinforcement experienced a buckling phenomenon in the first unconfined portion of the column above the 500 mm continuous wrapping (not well visible in Fig.9a because hidden by the cracked resin layer). Furthermore, under high values of the imposed displacement, the efficiency of the SFRP reinforcement was compromised by the slip of thread connectors from the concrete stub (Fig. 9b).

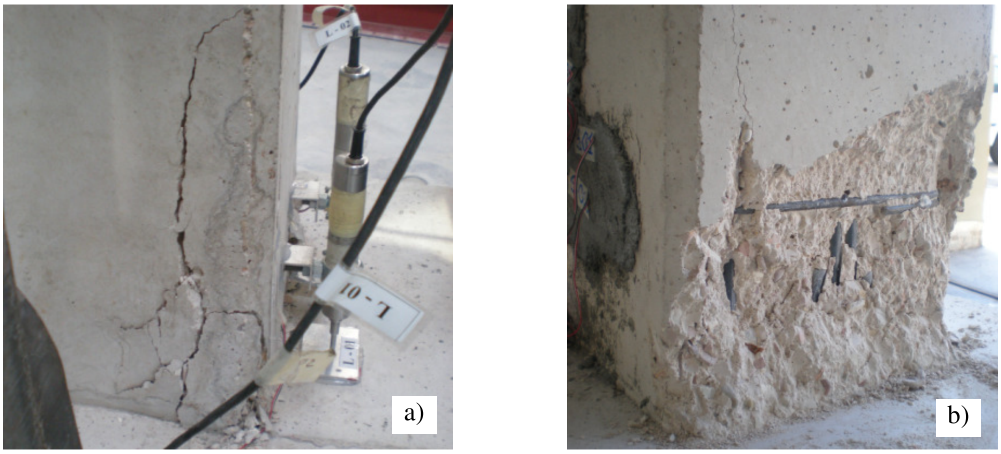

Figure 6. Unstrengthened column with "sufficient" steel reinforcement detailing (US1).

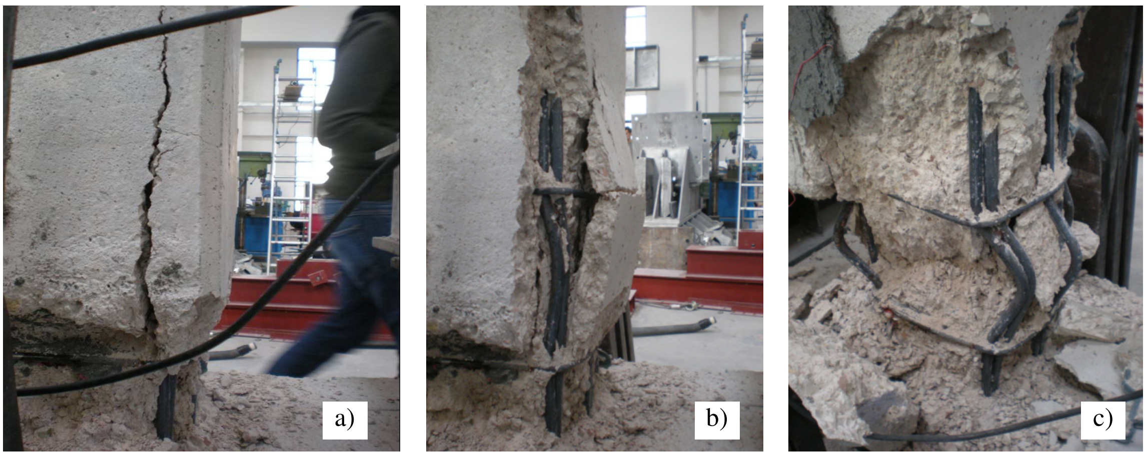

Figure 7. Unstrengthened column with "insufficient" steel reinforcement detailing (US2).

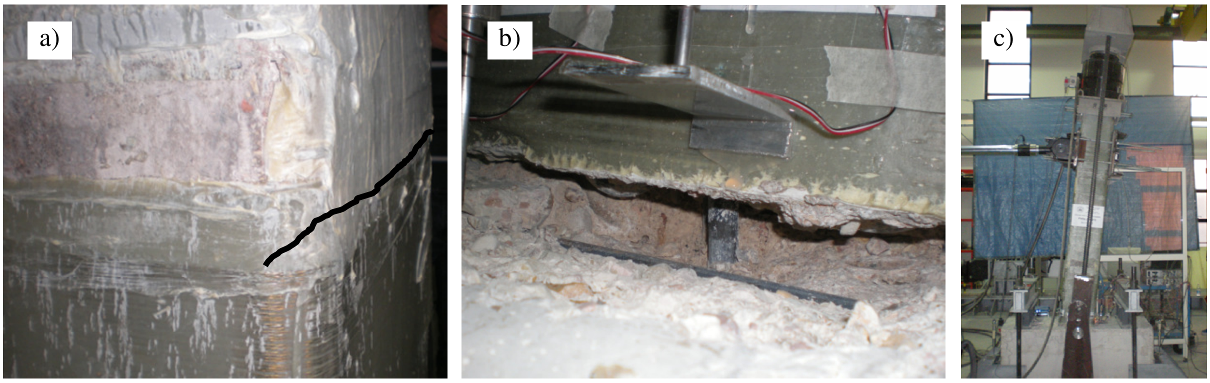

Figure 8. Column with "sufficient" steel reinforcement and confined with "type A" SFRP system (A1).

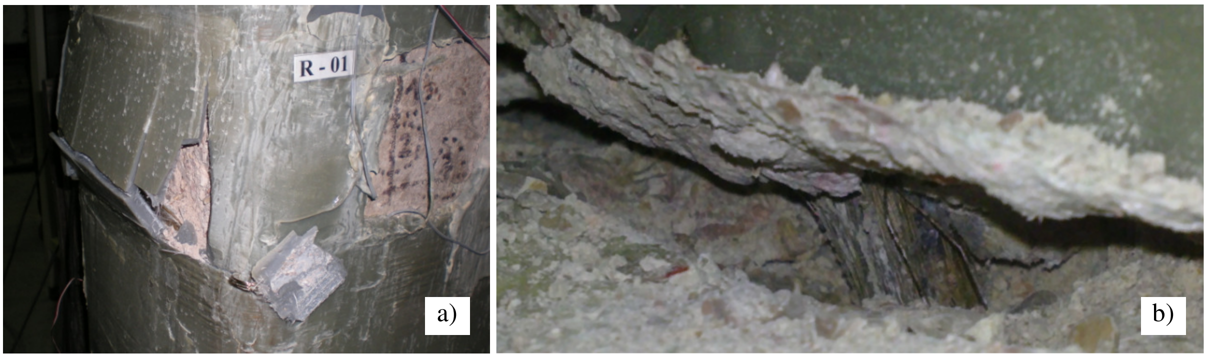

Figure 9. Column with "insufficient" steel reinforcement and strengthened with "type B" SFRP system (B2).

3.3 Stiffness degradation and energy dissipation

Based on the experimental results, it was possible to evaluate the mean value of stiffness for the i-th cycle by using the following ratio (Mayes and Clough 1975):

$$k = \frac{\left|F^{+}_{max,i}\right| + \left|F^{-}_{max,i}\right|}{\left|\Delta^{+}_{max,i}\right| + \left|\Delta^{-}_{max,i}\right|} \tag{3.2}$$

The stiffness of each displacement cycle k was then normalized with respect to that of the first cycle k_I, thus providing a measure of the stiffness degradation.
The relationships between k/k_I and drift ratio are plotted in Fig. 10a. As shown, the unstrengthened column with "insufficient anchorage" steel reinforcement (US2) exhibited a greater rate of stiffness degradation than the counterpart US1. This may be related to: a) low concrete strength of the column US2; b) reduced concrete-steel bond due to the non-optimal anchorage detailing used for steel rebars (i.e. lack of end-hooks; inadequate lap-splice length).
The stiffness degradation is practically independent on the presence of SFRP external confinement; in fact, under low displacement values, the curves relative to specimens A1 and US1 overlap each other.
Conversely, the improved behavior is evident for the column B2; in this case, the use of a strengthening *"type B"*, although performed on a member with "insufficient anchorage" detailing, also allowed to increase the member stiffness.
Finally, Fig. 10b depicts the relationships between the cumulative dissipated energy ($E\mu$) and the imposed drift ratio. In order to by-pass the dependence on the concrete strength level, this energy parameter was calculated – at each imposed displacement – from the area under the normalized flexural strength (μ)-Δ response enclosed within one complete cycle.
As shown, under low deformation cycles, the energy dissipated by all the members is approximately the same. By increasing the drift ratio, the column B2 dissipates more energy than the counterpart A1;

however, if the cumulated energy is computed up to the conventional collapse of each member, it can be observed that the two columns approximately dissipate the same amount of energy (the conventional collapse is anticipated in the case of the member B2 as shown in Table 2).

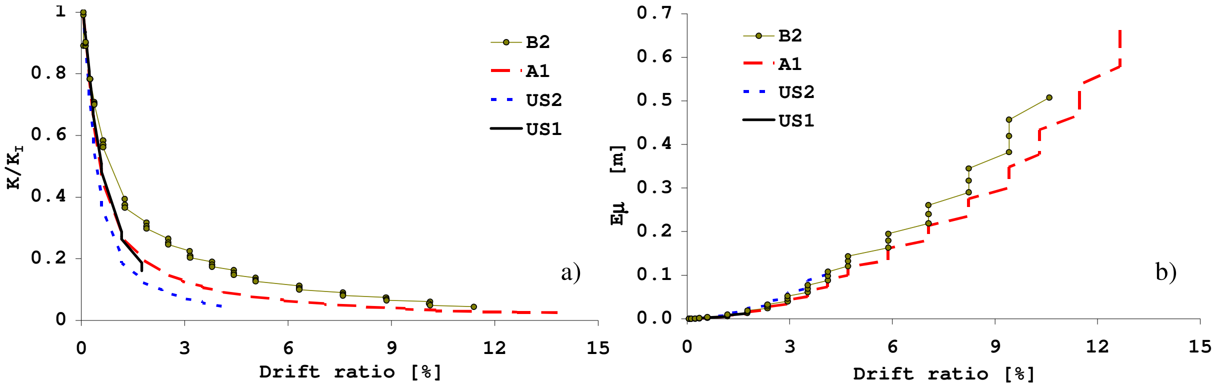

Figure 10. Stiffness degradation (a); energy dissipation (b).

4. CONCLUSIONS

This paper has presented the first results of an experimental campaign undertaken to investigate the seismic behaviour of full scale RC columns externally strengthened with SFRP systems. The first performed tests, all relative to square (300x300 mm) columns, have shown that the cyclic behaviour of SFRP confined members is mainly characterized by a rigid rotation due to the slippage and elongation of steel rebars at the column-stub interface where a wide crack is located. Compared with a member wrapped with four carbon FRP layers, the SFRP confined column is able to exhibit significantly higher displacements although also in this case the strength increase is rather limited. The combined use of SFRP confinement and longitudinal reinforcement anchored to the foundation allows to obtain an appreciable increase of strength though lower than that achievable by using CFRP confinement and steel profiles. The reduced performance is also due to the premature loss of efficiency of the longitudinal SFRP reinforcement caused by the slip of thread connectors from the concrete stub.

AKCNOWLEDGEMENT

The Authors gratefully acknowledge “Fidia S.r.l. - Technical Global Services, Perugia, Italy” for the financial support to the experimental program and the realization of the SFRP strengthening systems.

REFERENCES

Abdelrahman, K. and El-Hacha, R. (2011). Behavior of Large-Scale Concrete Columns Wrapped with CFRP and SFRP Sheets. *J. of Composites for Construction.* (in print) *doi:10.1061/(ASCE)CC.1943-5614.0000278.*

American Concrete Institute, ACI (2008). Guide for the Design and Construction of Externally Bonded FRP Systems for Strengthening Concrete Structures. *ACI 440.2R-08*. Farmington Hills, Mich.

CNR-DT200 (2004). Guide for the Design and Construction of Externally Bonded FRP Systems for Strengthening Existing Structures. CNR, National Research Council, Rome, Italy.

El-Hacha, R. and Mashrik, M. A. (2012). Effect of SFRP confinement on circular and square concrete columns. *Engineering Structures* **36**, 379–393.

Fédération internationale du Béton, fib (2001). Externally bonded FRP reinforcement for RC structures. Bulletin No. 14, Technical Rep. Lausanne, Switzerland.

Mayes, R.L. and Clough, R.W. (1975). State of the art in seismic shear strength of masonry – An evaluation and review. *EERC Report*, Berkeley, California, USA.

Realfonzo, R. and Napoli, A. (2009). Cyclic behavior of RC columns strengthened by FRP and steel devices. *Journal of Structural Engineering* **135:10**, 1164–1176.

Realfonzo, R. and Napoli, A. (2011). Concrete confined by FRP systems: Confinement efficiency and design strength models. *Composites: Part B* **42**,736–755.

Teng, J.G., Chen, J.F., Smith, S.T. and Lam, L. (2002). FRP–strengthened RC structures, Wiley, U.K.